



Molecular Crystals and Liquid Crystals Science and Technology. Section A. Molecular Crystals and Liquid Crystals

Publication details, including instructions for authors and
subscription information:

<http://www.tandfonline.com/loi/gmcl19>

Structures of Point Integer Disclinations and Their Annihilation Behavior in Thermotropic Liquid Crystal Polyesters

Ding-Kuo Ding^a & Edwin L. Thomas^a

^a Department of Materials Science and Engineering, MIT,
Cambridge, MA, 02139

Version of record first published: 24 Sep 2006.

To cite this article: Ding-Kuo Ding & Edwin L. Thomas (1994): Structures of Point Integer Disclinations and Their Annihilation Behavior in Thermotropic Liquid Crystal Polyesters, Molecular Crystals and Liquid Crystals Science and Technology. Section A. Molecular Crystals and Liquid Crystals, 241:1, 103-117

To link to this article: <http://dx.doi.org/10.1080/10587259408029748>

PLEASE SCROLL DOWN FOR ARTICLE

Full terms and conditions of use: <http://www.tandfonline.com/page/terms-and-conditions>

This article may be used for research, teaching, and private study purposes. Any substantial or systematic reproduction, redistribution, reselling, loan, sub-licensing, systematic supply, or distribution in any form to anyone is expressly forbidden.

The publisher does not give any warranty express or implied or make any representation that the contents will be complete or accurate or up to date. The accuracy of any instructions, formulae, and drug doses should be independently verified with primary sources. The publisher shall not be liable for any loss, actions, claims, proceedings, demand, or costs or damages whatsoever or howsoever caused arising directly or indirectly in connection with or arising out of the use of this material.

Structures of Point Integer Disclinations and Their Annihilation Behavior in Thermotropic Liquid Crystal Polyesters

DING-KUO DING and EDWIN L. THOMAS

Department of Materials Science and Engineering, MIT, Cambridge, MA 02139

(Received October, 1992; in final form May 6, 1993)

A schlieren texture composed of integer strength point disclinations has been observed in a thermotropic liquid crystal polymer. The director patterns about positive and negative disclinations are studied by optical microscopy and scanning electron microscopy. Defects are located at the specimen-air interface and occur due to the different boundary conditions of the liquid crystal at the air and glass interfaces. The annihilation behavior of these integer defects, created by a temperature-drop procedure from an initial isotropic state into the nematic state, was also investigated. It was found the relation between pair separation, D , and annihilation time, t_0 , was $D \propto (t_0 - t)^{0.5}$, which was in good agreement with the recent scaling solution prediction by Pargellis *et al.*¹

Keywords: disclinations, defect dynamics, annihilation

INTRODUCTION

In recent years scientists and engineers have become interested in thermotropic liquid crystal polymers because of their attractive properties, combining virtues from polymers and from liquid crystals. Their unusual physical properties have made them exciting materials for fundamental research. The schlieren textures of liquid crystals are easily visible under an optical microscope. These textures essentially originate from rotational defects in the orientationally ordered liquid. Defects and textures are well described in the monographs by Demus and Richter² and by Kléman.³ In nematic phases there are two main kinds of rotational defects: line and point disclinations. Defects are characterized by their strength, s , defined by the total change of the orientation of the director in a circuit around the singularity divided by 2π . A positive (negative) value of strength corresponds to the case which the circulatory direction and the rotational direction of director are the same (opposite). The director distortions involved in point disclinations are three dimensional, whereas line disclinations in thin films produce a two dimensional distortion. Most line disclinations found in liquid crystals are half-integer defects due to their more favorable energetic state. However, integer defects with nonsingular cores due to director escape in the third dimension may be found in thin capillaries.⁴

A typical procedure to create defects in a liquid crystal is to use symmetry breaking via the phase transition from the disordered isotropic phase to the ordered phase by varying the temperature or pressure.⁵ DeGennes⁶ has also described a way to create point defects by applying a magnetic field normal to the liquid crystal free surface or to the interface between the nematic and isotropic phase with a homogeneous or conical boundary condition. Meyer⁷ has studied point disclinations at the upper air surface in a nematic small molecule liquid crystal (SMLC). A regular network of point disclinations in a SMLC without a magnetic field has been observed,⁸ in which the homeotropic boundary condition at the glass-specimen interface played the role of the magnetic field in deGennes' description. Point defects may also be found along the central axis of a glass tube.^{1,4,9} The orientation at the glass boundary is approximately homeotropic while it is approximately homogeneous in the center of the tube.

Integer strength disclinations in thermotropic liquid crystal polymers have seldom been reported or commented upon, although several published images reveal their presence.^{10,11} In this paper, we describe the nature of integer point defects in a thermotropic liquid crystal polyester produced simply by changing temperature through the isotropic-nematic phase transition. The sign of the integer defects is determined using a first order red plate or a quarterwave plate under polarized light. Their detailed director structures are revealed via the lamellar decoration technique¹² with optical microscopy and scanning electron microscopy. In addition to the structure of defects, we also study the defect dynamics. Defect dynamics in liquid crystals has recently become an important issue since the defect strings provide a laboratory system to test the "one-scale" model for cosmic string evolution.⁵ Only a few investigations have reported the dynamic behavior of defects in polymeric or in small molecule liquid crystals.^{1,13-15} Recently, a small molecule liquid crystal, 4-cyano-4'-*n*-pentylbiphenyl, was used to study the dynamic behavior of integer point defects, created by an order-disorder phase transition.¹ The pair annihilation and coarsening behaviors of the schlieren texture of our polymeric liquid crystal samples were similar to the SMLC scaling-solution prediction.

EXPERIMENTAL

The material used in this study is a main chain semi-flexible thermotropic liquid crystal polyester based on 1,10-decane bisterephthaloyl chloride with methyl hydroquinone (MHDT). This polymer was synthesized at Cornell University with the help of Prof. C. Ober, and its synthesis and characterization are described in more detail in Reference 16. The transition temperatures are $T_{cn} = 145^{\circ}\text{C}$ and $T_{ni} = 170^{\circ}\text{C}$. Repeated DSC traces demonstrate that MHDT is relatively chemically stable under thermal cycling up to approximately 200°C . This stability makes it possible to conduct nematic-isotropic transitions by thermal cycling, whereas most liquid crystal polymers become unstable when they approach their isotropic (clearing) temperature.

A thin polymer film about $10\text{ }\mu\text{m}$ thick was prepared in the melt state by blade shearing on a glass slide. The glass slide is first cleaned with chloroform in an

ultrasonic bath, followed by immersion in a stirred solution of hydrogen peroxide/ammonia/water (1:1:5 mixture) at 70°C. The glass slide is then washed by water and dried by nitrogen gas. After blade shearing, the polymer film sample, whose top surface is free, is placed in a Linkam hot stage and heated into the isotropic state (180°C). The temperature was then quickly dropped to 160°C which is just below the isotropic-nematic transition temperature⁷ to create a large number of defects. The sample was then kept at constant temperature to allow some defect annihilation for easier examination. These defect textures could be captured by slow cooling or by quenching the sample into room temperature water. To directly visualize the defect structures, the samples were then annealed for a short time at a temperature 25°C below melting temperature. During annealing, the quenched glassy nematic polymer partially crystallizes into a lamellar morphology, where the director of the remaining glassy liquid crystal is normal to the lamellae. The lamellae serve to decorate the underlying molecular arrangement of the frozen nematic.¹² Finally, for good contrast in SEM, the sample was etched with 40 wt% methylamine in water¹⁷ and coated with Au and viewed in secondary electron imaging mode (SEI) with a Cambridge Instruments SEM at 5 KeV. To study the defect annihilation behavior, the whole process, including the defect creation and the coarsening of schlieren textures at constant temperature (160°C), was recorded in situ using a Zeiss optical microscope (OM) equipped with Javelin video camera.

RESULTS AND DISCUSSION

Defect Structures

Defects in liquid crystals cause abrupt changes of the director field resulting in elastic distortion of the director configuration near them. Defects prefer to form in pairs of opposite sign to compensate long range elastic distortion, known as splay cancellation. A defect pair (dipole pair) will tend to approach one another until they annihilate to minimize the total energy. A stable dipole pair may be formed by an air bubble (which acts as a positive integer defect) compensating a negative integer point defect.⁷

A typical schlieren texture of integer strength defects is shown in Figure 1, which is very similar to the defect textures in SMLCs. The schlieren textures produced by the temperature-drop defect creation procedure are different each time, that is, the defects are randomly created. The sign of each defect can be determined by rotating the crossed polars. The defects do indeed form in negative-positive pairs, which can be confirmed by tracing the connecting brushes.

From continuum theory,¹⁸ assuming the director is confined to the xy -plane, the energy of an individual defect is proportional to s^2 . Defects of strength $|s| > \frac{1}{2}$ should be unstable and dissociate into $|s| = \frac{1}{2}$ defects. Dzyaloshinskii¹⁹ has shown that a $s = 1$ concentric line defect is stable only if $k_{22} > 2k_{33}$ and $k_{11} > k_{33}$. It is expected that the $s = 1$ line defect occurs only rarely in typical nematics because of the usual small value of the twist elastic constant k_{22} .

Disclinations of integer strength are always formed in our experiments. We believe this kind of schlieren texture of *only* integer defects in a main chain ther-

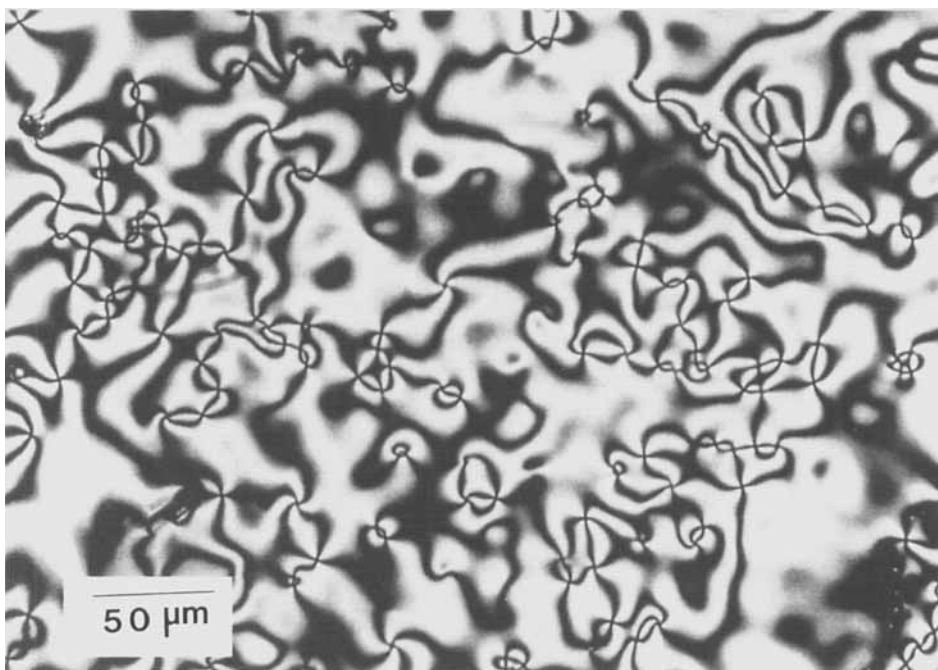


FIGURE 1 OM of schlieren texture of MHDT film created by quenching the sample from the isotropic (180°C) state to the nematic (160°C) state. The points with four brushes indicate the presence of integer defects of $s = \pm 1$. See Color Plate III.

motropic liquid crystal polymer has not been previously reported. These integer defects are point defects which arise in the present case due to the particular boundary conditions at the air interface (homogeneous) and at the glass interface (homeotropic) (see schematic Figure 2). Whether or not a singular line integer defect is stable or “escapes” to a point defect for this thermotropic polyester material is unknown at present. Attempts at producing a radial $s = +1$ line defect in a glass capillary with homeotropic conditions were unsuccessful due to sample handling difficulties.

To prove an approximate homeotropic condition with the glass surface, a thin film was made between two glass slides. If homeotropic conditions occur at both glass-specimen boundaries, then the sample will not show any birefringence through crossed polars since in this arrangement the molecular axes are along the optical axis (uniaxial). Apparent zero birefringence is indeed observed for samples between two glass slides and this oriented nematic state can be distinguished from the isotropic state by simply pressing on the cover glass causing some nonaxial orientation, which causes the dark nematic region to brighten immediately. The approximately homogeneous condition at upper free surface can be shown by the edge-on lamellar orientation described next.

To directly visualize the director pattern at the upper (air) sample surface at high resolution, the lamellar decoration and etch technique is used.^{12,17,20} The director field (molecular axes) is revealed in SEM images by the pattern of crys-

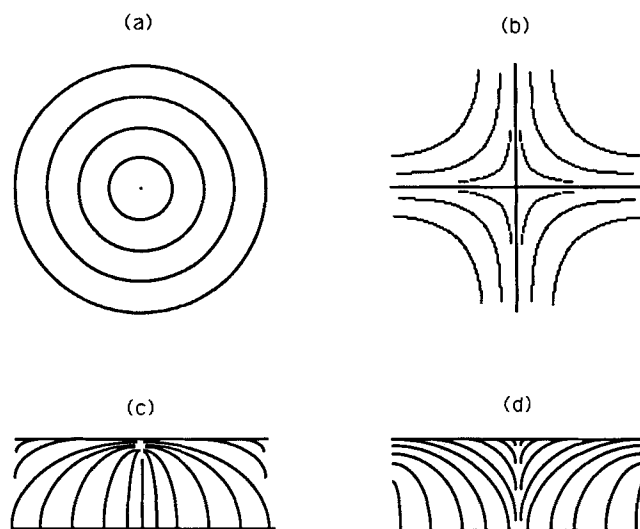


FIGURE 2 Schematic of the integer defects structure.⁷ (a) and (b) show the top view, (c) and (d) show the side view.

talline lamellae (~ 15 nm thick), which are formed by crystallization during the quench or upon sample annealing. TEM and electron diffraction prove that the molecular axes are normal to the lamellae so the director pattern is the set of trajectories orthogonal to the pattern of lamellae, which means the molecular axes are in the plane of the film at the upper free surface. To enhance SEI contrast an amine etch is used. The ester linkages in MHDT are cleaved by the amine and the etching rate of noncrystalline glassy nematic regions between the lamellae is faster than that of the crystalline lamellae. Therefore, the edge-on lamellae protrude from the polymer surface such that the director fields can be imaged by SEI in the SEM (or by TEM of surface replicas²¹).

Optical microscopy may be used to determine the sign of the integer defects. Figure 3 is a crossed-polars OM image of radial ($s = +1$) and hyperbolic ($s = -1$) defects. Stripes result from sample crystallization into bundles of parallel oriented lamellae during the cooling process, and the different interference colors arise from regions of different sample thickness. A low magnification OM of the schlieren texture fields is shown in Figure 4a. Figure 4b is an SEM micrograph showing better detail of director patterns around integer defects. The individual integer defect structures of $s = +1$ and $s = -1$ are clearly evident in the pattern of the lamellae. Since the molecular axes are normal to the lamellae, the schematic inserts show the actual director patterns.

When either a quarterwave plate or a first order red (Red I) plate is employed with the differential interference contrast mode, image contrast increases and yellow and blue regions will be present, depending on the local orientation and film thickness. Such color images are useful to determine the approximate orientation of the molecular axis from birefringent interference figures, which correspond to the fast and slow directions of the transmitted light. For a quarterwave plate, if the fast component in the sample and quarterwave plate are parallel, the total path

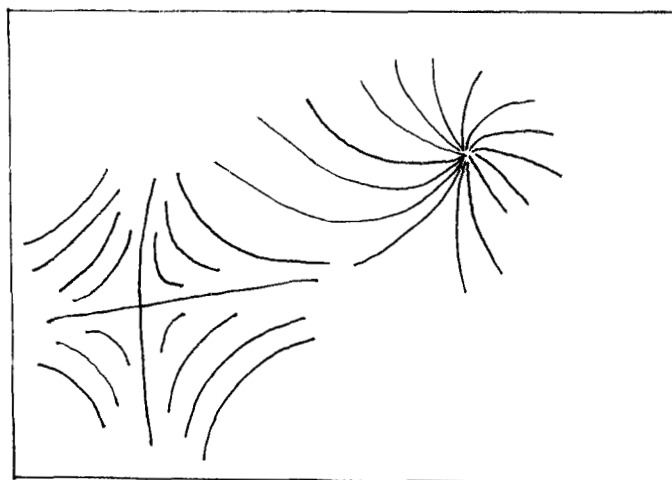
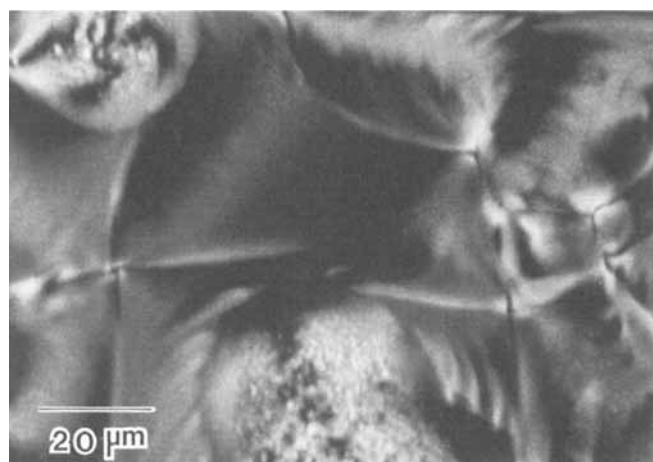


FIGURE 3 OM of integer defects of MHDТ quenched from the nematic state into room temperature water. The stripes resulted from sample crystallization during the cooling process. See Color Plate IV.

difference is increased, and the interference color goes up scale, perhaps to yellow. If the fast component of the sample is parallel to the slow component of the plate, the interference color goes down to blue. The reverse occurs for insertion of a Red I plate, i.e. the color shows blue if the fast components in the sample and the plate are parallel, while showing yellow if the slow component of the sample is parallel to the fast component of the plate.

Usually the fast component of transmitted light (smaller index of refraction) is along the main chain molecular axis, thus it is easy to identify the approximate orientation of the molecules. Figure 5 shows the interference image of the schlieren texture using a Red I (Figures 5a, 5b) or a quarterwave (Figure 5c) plate. For the $s = +1$ defect, since the director field is symmetrical around the defect, when the sample is rotated 45° , the interference color does not change, while the interference

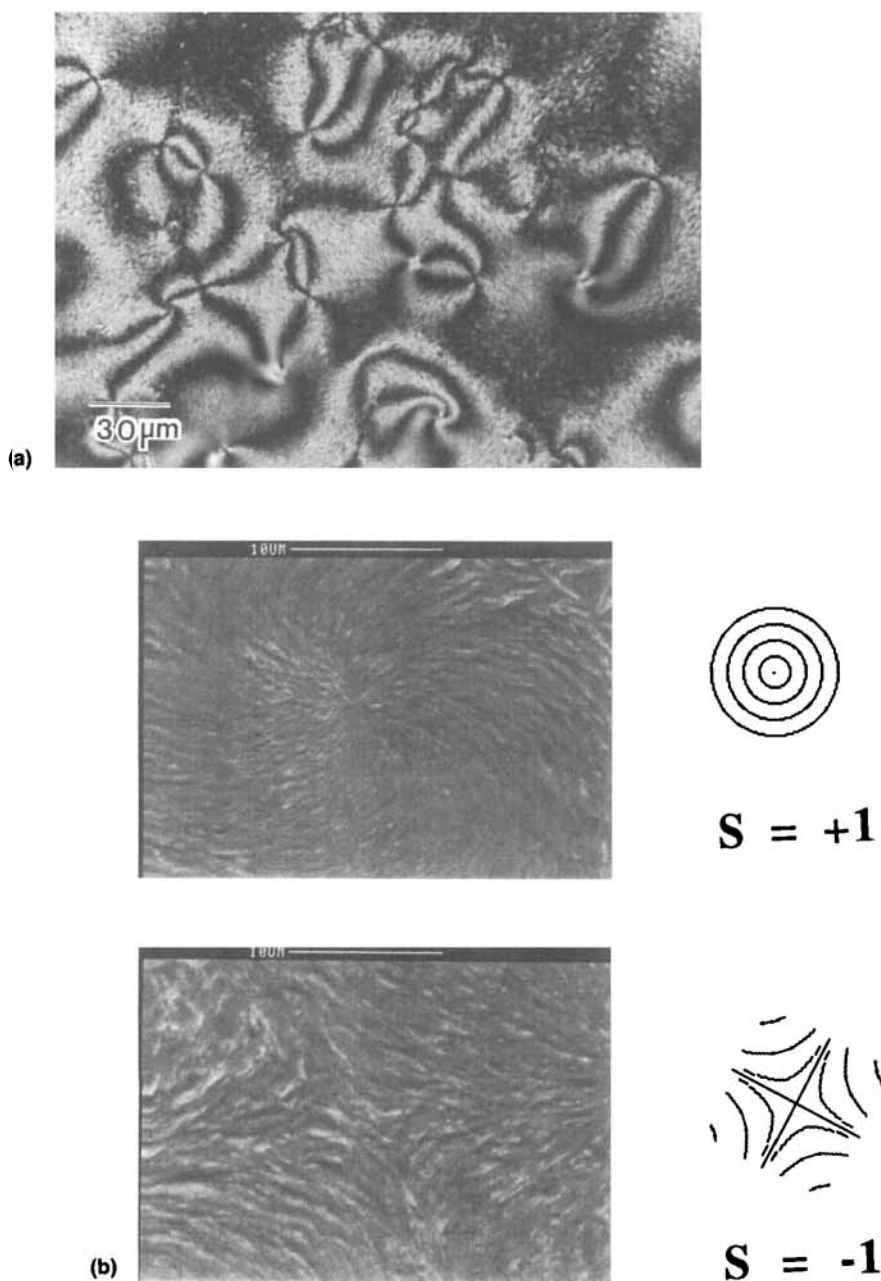


FIGURE 4 (a) OM of MHDt quenched to room temperature, and annealed at 120°C for 15 minutes, and etched in 40 wt% methylamine/water solution for 20 minutes. (b) SEM of the etched sample in Figure 4a showing the detailed director fields of a positive integer defect and negative integer defect. The director fields of the schlieren texture are directly seen due to lamellar decoration. See Color Plate V.

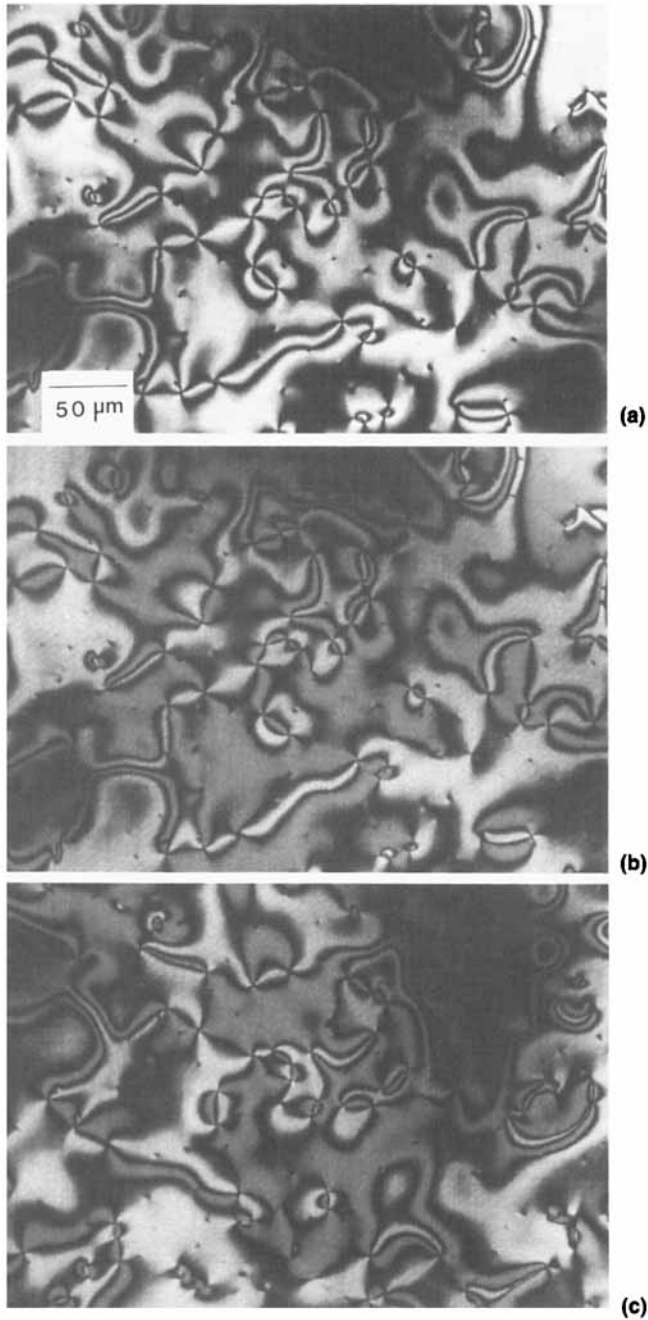
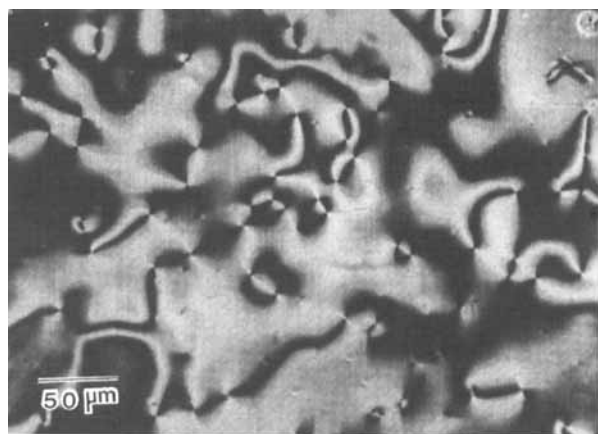
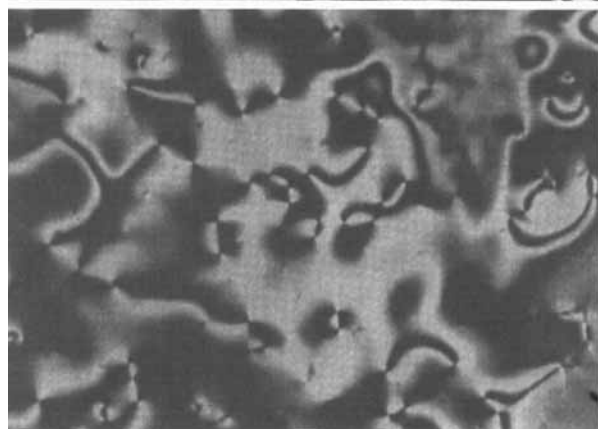


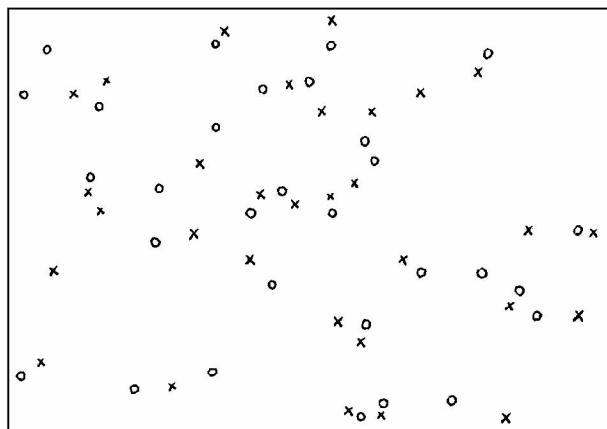
FIGURE 5 (a) The schlieren texture under cross polars. (b) The schlieren texture with first order red plate. (c) Sample stage rotated 45° from (b). (d) The schlieren texture with quarterwave plate. (e) Defects are identified by positive and negative sign. See Color Plate VI.



(d)



(e)



O positive
x negative

FIGURE 5 (continued). See Color Plate VI continued

PAIR ANNIHILATION



t = 255 sec



t = 176 sec



t = 116 sec



t = 11 sec

FIGURE 6 A typical pair annihilation sequence with experimental time shown on the left side. A pair of defects are pinned at the right side. See Color Plate VII.

color of the $s = -1$ rotates around the defect (Figures 5a and 5b). One way to identify $s = -1$ defects is to find points whose blue color crosses two quadrants, which indicates the asymptotic axes of the defect lie between the polarizer and analyzer directions. Once one defect is identified, it is easy to determine the sign of an adjacent defect by tracing the brushes connecting the opposite sign defect. In our samples, if a Red I plate is inserted, the interference color of $s = +1$ defects is blue for the second and fourth quadrants, which means the molecular axes are approximately tangential about the defect center. This is consistent with SEM which shows radial lamellae near the disclination core corresponding to a concentric molecular director pattern about the defect. The $s = +1$ defects are thus approximately pure bend, suggesting $k_{11} > k_{33}$ for this TLCP. Hudson and Thomas²¹ previously measured the elastic anisotropy ϵ , $\epsilon = (k_{11} - k_{33})/(k_{11} + k_{33})$ of this same polyester and found $k_{11} = 1.5k_{33}$ in agreement with the concentric (easy bend) $s = +1$ defect director pattern in Figure 4b. Points with blue color in the first quadrant can be identified as $s = -1$ defects.

ANNIHILATION BEHAVIOR

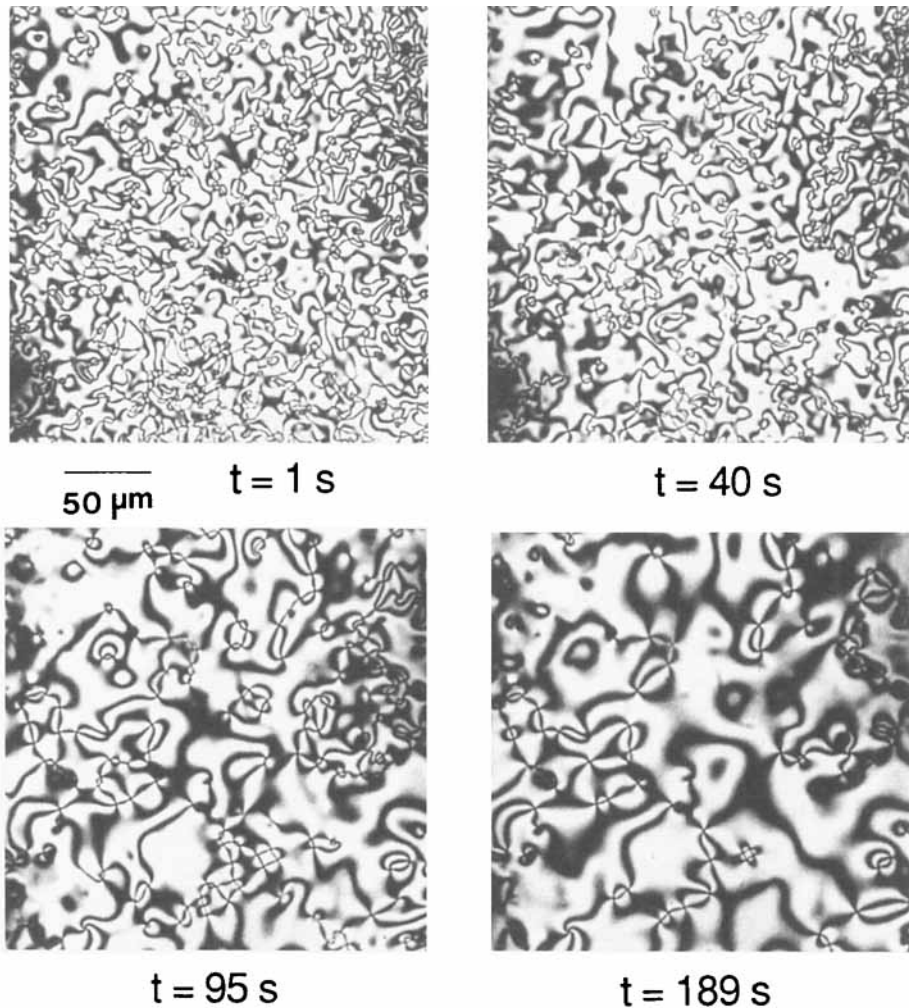


FIGURE 7 OM between crossed polars of overall isothermal coarsening sequences of schlieren textures, created by a thermal quench. See Color Plate VIII.

Annihilation Behavior

Defects of opposite sign tend to attract each other until they annihilate to minimize the distortional energy. Figure 6 shows a typical pair annihilation sequence which occurs during isothermal coarsening of the schlieren texture. In this case the positive defect seems to move faster than the negative one, but the reverse effect was also found with other defect pairs. Figure 7 shows a sequence of schlieren textures between crossed polarizers during the isothermal coarsening process. A square quad-defect was formed (lower-center region of micrograph) and the shape is

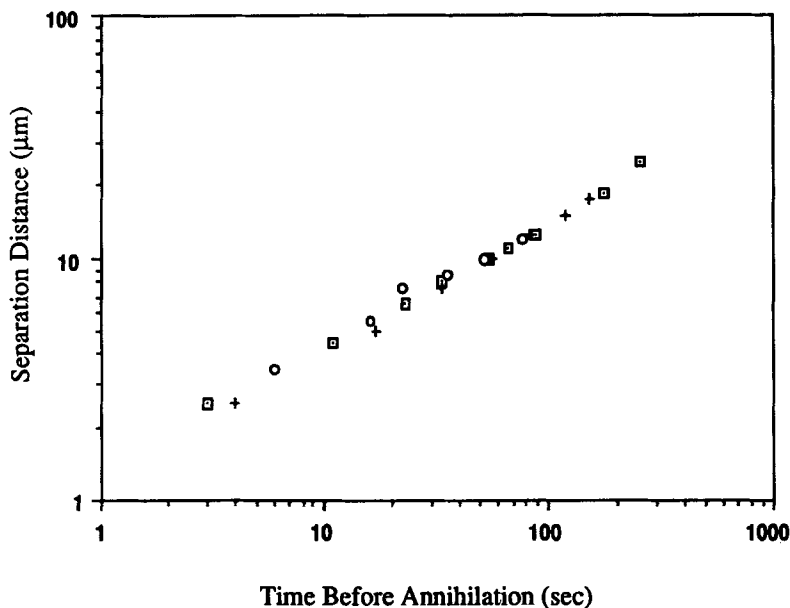


FIGURE 8 The pair distance D vs time before annihilation for three sets of data. The slope fits the scaling prediction by Pargellis *et al.*¹

maintained during annihilation. This implies the velocity of both positive and negative integer defects is similar. Such a symmetric arrangement of four disclinations (two positive, two negative) was depicted in Lehmann's 1918 monograph.²² A similar zero net dipole arrangement of four half integer defects has been identified in both flow and magnetic field oriented TLCPs.²³

The variation of defect mobility may be due to some impurities, or the presence of lower or higher molecular weight polymer around the core area of the defects impeding the movement of defects. Mazelet and Kléman²⁴ have noted the movement of $s = -\frac{1}{2}$ defects is faster than the movement of $s = +\frac{1}{2}$ defects, which they suggest may be due to an excess concentration of chain ends at the disclination core for the $+\frac{1}{2}$ defects.

Recently, experimental and theoretical investigations have concerned the time evolution of both the number density of defects, $\rho(t)$, and the separation distance between opposite signed defects, $D(t)$. By assuming that the approach velocity depends inversely on the defect separation distance, Pargellis *et al.*¹ predicted $D(t)$ is given $(t_0 - t)^{0.5}$, where t_0 is the time to annihilation. Considering the number density of the defects and the average separation distance of a pair-defect, these two quantities can be related by $D \propto \rho^{-1/d}$, where d is the spatial dimensionality. In the two dimensional case, defects move within the plane, therefore, the number density is scaled by the annihilation time as $\rho(t) \sim t^{-1}$. An earlier model by Dreizin and Dykhne²⁵ also produces a $D(t) \propto (t_0 - t)^{0.5}$ behavior by assuming that the attractive interaction between defects is balanced by the retarding viscous force.

Pargellis *et al.*¹ found $D(t) \propto (t_0 - t)^{0.5}$ behavior at large times for point defects induced in a SMLC via pressure jumps or thermal quenches. A similar result for

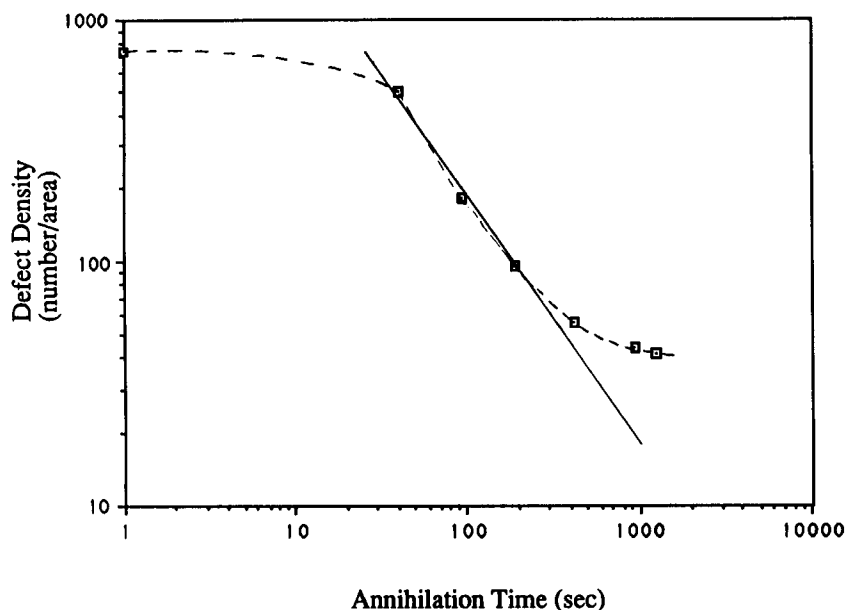


FIGURE 9 Defect density vs annealing time at 160°C using data as in Figure 7.

the defect pair separation was observed in films for which the thickness exceeds the typical separation distance.²⁶ However, other experimental results yielded $D(t) \propto (t_0 - t)$ behavior for samples which the thickness was much less than pair separation distance.^{1,27} A different experimental power law, $D \propto t^{0.35}$ was determined by Shiwaku *et al.*²⁸ in a liquid crystal polymer system containing predominantly half-integer defects with the average defect separation distances larger than polymer film thickness (1 μm).

Three data sets of separation distance D against time before annihilation (one from Figure 6) are plotted in Figure 8. The scaling relation between separation distance and annihilation time is approximately $D \propto (t_0 - t)^{0.5}$, where separation distances are from 1–30 μm and the film thickness is around 10 μm . It is straightforward but somewhat tedious to count the total number of defects in our system, especially at the beginning of the annihilation process. Figure 9 shows as the number of defects decreases with time, the average distance between neighboring defects increases. The data fit the anticipated t^{-1} power law for times between 30 seconds and 500 seconds. At longer times, we find a tail effect. This tail effect results from pinned defects due to impurities or lower molecular weight material still in the isotropic state at the temperature of observation (160°C). These motionless defects are always accompanied by a defect of opposite sign, as noted by Meyer.⁷

SUMMARY

We have described a simple way to create integer point defects and to study the annihilation behavior of these defects in a thermotropic liquid crystal polyester.

The schlieren texture comprised of only integer strength ($s = \pm 1$) defects was created by thermal quenching from the isotropic state to the nematic state. The detailed director patterns around defect nuclei were observed by scanning electron microscopy using the lamellar decoration technique. The defects are identified as point disclinations arising due to the different boundary conditions, one (homogeneous) at the free surface and one (homeotropic) at the glass-polymer interface. The schlieren textures are statistically reproducible with thermal cycling. In addition to the method of rotation of cross polars to determine the sign of the disclinations, the first order red plate and quarterwave plate methods were also used to determine the sign of integer point disclinations. The dynamic behavior of defects in liquid crystals, which is related to topological defects in the universal view, was also investigated. The annihilation behavior of defect pairs in our sample is similar to that for point defects in small molecule liquid crystals.^{1,26} The pair separation distance decreases with annihilation time t_0 as $D \propto (t_0 - t)^{0.5}$. The coarsening behavior of schlieren textures from experimental results are in good agreement with the scaling prediction⁵ of asymptotic behavior of disclination density $\rho(t) \propto t^{-1}$.

Acknowledgment

The authors would like to thank Professor C. K. Ober of Cornell University for helping with synthesis of the polymer and Prof. M. Kléman for useful discussions. This research was supported by NSF grants DMR-9214853 and DMR-9201845 (Polymers Program).

References

1. A. Pargellis, N. Turok and B. Yurke, *Physical Review Letters*, **67**, 1570 (1991).
2. D. Demus and L. Richter, *Textures in Liquid Crystals* (Verlag Chemie, New York, 1978).
3. M. Kléman, *Points, Lines, and Walls* (Wiley, Chichester, 1983).
4. P. E. Cladis and M. Kléman, *J. Phys., Paris*, **33**, 591 (1972).
5. I. Chuang, R. Durrer, N. Turok and B. Yurke, *Science*, **251**, 1336 (1991).
6. P. G. DeGennes, *The Physics of Liquid Crystals* (Clarendon Press, Oxford, 1974).
7. R. B. Meyer, *Mol. Cryst. Liq. Cryst.*, **16**, 355 (1972).
8. N. V. Madhusudana and K. R. Sumathy, *Mol. Cryst. Liq. Cryst.*, **129**, 137 (1985).
9. A. Saupe, *Mol. Cryst. Liq. Cryst.*, **7**, 59 (1973).
10. G. Galli, M. Laus, A. S. Angeloni, P. Ferneti and E. Chiellini, *Eur. Polym. J.*, **21**, 727 (1985).
11. P. LeBarny, J. C. Dubois, C. Friedrich and C. Noel, *Polym. Bull.*, **15**, 341 (1986).
12. E. L. Thomas and B. A. Wood, *Faraday Discuss. Chem. Soc.*, **79**, 229 (1985).
13. T. Shiwaku, A. Nakai, H. Hasegawa and T. Hashimoto, *Polymer Communications*, **28**, 174 (1987).
14. P. E. Cladis, W. van Saarloos, P. L. Pinn and A. R. Kortan, *Phys. Rev. Lett.*, **58**, 222 (1987).
15. S. Rojstaczer and R. S. Stein, *Mol. Cryst. Liq. Cryst.*, **157**, 293 (1988).
16. S. Antoun, R. W. Lenz and J. I. Jin, *J. Polymer Sci. Polym. Chem. Ed.*, **19**, 1901 (1981).
17. S. J. Organ and P. J. Barham, *Polymer Preprints*, **29**, 602 (1988).
18. F. C. Frank, *Disc. Faraday Soc.*, **25**, 19 (1958).
19. I. E. Dzyaloshinskii, *Sov. Phys. JETP*, **31**, 773 (1970).
20. S. D. Hudson, D. L. Vezie and E. L. Thomas, *Makromol. Chem., Rapid Commun.*, **11**, 657 (1990).
21. S. D. Hudson and E. L. Thomas, *Physical Review Letters*, **62**, 1993 (1989).
22. O. Lehmann, *Die Lehre von den flussigen Krystallen* (Wiesbaden, Bergman, 1918).
23. S. D. Hudson and E. L. Thomas, *Physical Review A*, **44**, 8128 (1991).

24. G. Mazelet and M. Kléman, *Polymer*, **27**, 714 (1986).
25. Y. A. Dreizen and A. M. Dykhne, *Sov. Phys. JETP*, **34**, 1140 (1972).
26. A. S. Sonin, A. N. Dhuvyrov, A. A. Sobachkin and V. L. Ovchinnikov, *Sov. Phys. Solid State*, **18**, 1805 (1976).
27. O. D. Lavrentovich and S. S. Rozhkov, *JETP Letter*, **47**, 254 (1988).
28. T. Shiwaku, A. Nakai, H. Hasegawa and T. Hashimoto, *Macromolecules*, **23**, 1590 (1990).